Nonlinear Analysis: Hybrid Systems 24 (2017) 100–114

Contents lists available at ScienceDirect

Nonlinear Analysis: Hybrid Systems

journal homepage: www.elsevier.com/locate/nahs

Computation of periodic solutions in maximal monotone dynamical systems with guaranteed consistency

W.P.M.H. Heemels [a,*], V. Sessa [b,1], F. Vasca [c], M.K. Camlibel [d]

[a] Control Systems Technology group, Department of Mechanical Engineering, Eindhoven University of Technology, The Netherlands

[b] Instituto de Matemática Pura e Aplicada (IMPA), Brazil

[c] Department of Engineering, University of Sannio, Benevento, Italy

[d] Johan Bernoulli Institute for Mathematics and Computing Science, University of Groningen, The Netherlands

ARTICLE INFO

Article history:
Received 29 October 2015
Accepted 29 October 2016

Keywords:
Hybrid systems
Set-valued dynamical systems
Computational methods
Periodic solutions
Stability of nonlinear systems
Maximal monotonicity

ABSTRACT

In this paper, we study a class of set-valued dynamical systems that satisfy maximal monotonicity properties. This class includes linear relay systems, linear complementarity systems, and linear mechanical systems with dry friction under some conditions. We discuss two numerical schemes based on time-stepping methods for the computation of the periodic solutions when these systems are periodically excited. We provide formal mathematical justifications for the numerical schemes in the sense of consistency, which means that the continuous-time interpolations of the numerical solutions converge to the continuous-time periodic solution when the discretization step vanishes. The two time-stepping methods are applied for the computation of the periodic solution exhibited by a power electronic converter and the corresponding methods are compared in terms of approximation accuracy and computation time.

1. Introduction

Set-valued dynamical systems and differential inclusions play an important role in many branches of science and engineering [1]. An important concept in this context is the maximal monotonicity of the involved set-valued mappings. There is a large body of literature on the use of maximal monotonicity in mathematics [2–4], and in recent years this property was also exploited in the context of non-smooth dynamical systems and hybrid systems such as linear complementarity systems [5–10], linear relay systems [11,12], piecewise linear systems, projected dynamical systems [13–15], and applications including electrical networks with switching elements as in power converters [7,10,16–18], constrained mechanical systems [19,20], and systems with dry friction. In fact, in most of the above mentioned works non-smooth systems are perceived as the interconnection of a linear time-invariant (LTI) system and a static relationship described by a set-valued mapping, which turned out to be fruitful for the analysis. This perspective finds its origin in Lur'e systems, see, e.g., [21].

* Corresponding author.
E-mail addresses: m.heemels@tue.nl (W.P.M.H. Heemels), valentina.sessa@uerj.br (V. Sessa), vasca@unisannio.it (F. Vasca), kanat.camlibel@gmail.com (M.K. Camlibel).
[1] Universidade do Estado do Rio de Janeiro (UERJ), Brazil.

http://dx.doi.org/10.1016/j.nahs.2016.10.006
1751-570X/

In this paper, we also focus on non-smooth dynamical systems that arise from the interconnection of LTI systems and static set-valued mappings, although we will embed these systems in a general class of differential inclusions (DIs) that satisfy maximal monotonicity properties. The latter embedding has been used also in, e.g., [8,22,23], in which an essential assumption was the (strict) passivity of the LTI systems and the maximal monotonicity of the set-valued mapping, which imply that the resulting DIs indeed have maximal monotone right-hand sides. For this type of set-valued dynamical systems we consider the problem of numerical construction of periodic solutions when these systems are being periodically excited. Although many methods exist for numerical (forward) simulation of set-valued systems, see, e.g., the survey paper [24], numerical methods for constructing periodic solutions *including formal justifications* are limited. Therefore, we propose two numerical methods here for which such formal justifications can be given.

The first numerical method is based on time-discretization (time-stepping) [25–28] in combination with extensive simulation. This method relies on the asymptotic stability property of the searched periodic solution of the continuous-time system (and the asymptotic stability of the periodic solution of the discretized system) to warrant that sufficiently long numerical simulation recovers the periodic solution accurately. In fact, the property that we exploit is closely related to concepts such as incremental stability [29] (based on quadratic Lyapunov functions) and quadratic convergence [30,31]. As such, the work in this paper connects to results on (quadratic) convergence in the context of maximal monotone DIs such as, e.g., [32,33], and on incremental stability such as, e.g., [22] (although this terminology was not explicitly used in [22]). In fact, the concepts of quadratic convergence and Lyapunov-based characterizations for incremental stability can even be seen as a kind of maximal monotonicity properties in some situations (cf. Remark 1).

The second numerical method studied in this paper combines time-stepping techniques with two-point boundary value problems (to enforce periodicity), as used in, e.g., [34].

Both these classes of methods seem to work well in practice, but they often lack formal justification. Instead, in this paper, the numerical schemes are accompanied with a guarantee of *consistency*, in the sense that the 'exact' periodic solution (i.e., the one belonging to the continuous-time system) is recovered when the discretization period (and simulation window) tends to zero (and infinity, respectively). To the best of our knowledge, such proofs are not available in the literature. Building upon our preliminary work [35], in which no formal proofs were provided and more stringent conditions were needed, in this paper we do present *formal conditions under which the consistency can be guaranteed for both these methods (including rigorous proofs)* when applied to the class of non-smooth dynamical systems under study. Once the theoretical justification in the form of consistency is in place, we also provide a numerical example to illustrate the efficiency of the two methods and compare them in terms of approximation accuracy and required computation time.

The following notation will be used in the sequel. Closures and interiors of sets are denoted by cl and int. For a set-valued mapping $\mathcal{P} : \mathbb{R}^n \rightrightarrows \mathbb{R}^n$ we denote the domain of $\mathcal{P}$, i.e. $\{x \in \mathbb{R}^n \mid \mathcal{P}(x) \neq \emptyset\}$, by dom $\mathcal{P}$. The graph $\mathrm{gr}(\mathcal{P})$ of $\mathcal{P}$ is given by $\{(x, x^*) \in \mathbb{R}^n \times \mathbb{R}^n \mid x^* \in \mathcal{P}(x)\}$. The inverse mapping of $\mathcal{P}$ is denoted by $\mathcal{P}^{-1} : \mathbb{R}^m \rightrightarrows \mathbb{R}^m$ and defined as $\mathcal{P}^{-1}(y) = \{x \in \mathbb{R}^n | y \in \mathcal{P}(x)\}$. Note that in the context of set-valued mappings the inverse is always well defined. For the standard inner product in $\mathbb{R}^n$ and the corresponding norm, we write $\langle \cdot \mid \cdot \rangle$ and $|\cdot|$, respectively. A set-valued mapping $\mathcal{P} : \mathbb{R}^n \rightrightarrows \mathbb{R}^n$ is called monotone, if $\langle x^* - y^* \mid x - y \rangle \geq 0$ for all $(x, x^*) \in \mathrm{gr}(\mathcal{P})$ and all $(y, y^*) \in \mathrm{gr}(\mathcal{P})$. We call $\mathcal{P}$ maximal monotone, if $\mathcal{P}$ is monotone and there is no other monotone map $\mathcal{P}' : \mathbb{R}^n \rightrightarrows \mathbb{R}^n$ such that $\mathrm{gr}(\mathcal{P}) \subseteq \mathrm{gr}(\mathcal{P}')$ and $\mathrm{gr}(\mathcal{P}) \neq \mathrm{gr}(\mathcal{P}')$. See [2–4] for more details.

2. Problem formulation

Given matrices $A \in \mathbb{R}^{n\times n}$, $B \in \mathbb{R}^{n\times m}$, $C \in \mathbb{R}^{m\times n}$, $D \in \mathbb{R}^{m\times m}$ and a set-valued map $\mathcal{M} : \mathbb{R}^m \rightrightarrows \mathbb{R}^m$, we are interested in the (possibly non-smooth) dynamical system

$$\dot{x}(t) = Ax(t) + Bz(t) + u(t) \tag{1a}$$

$$w(t) = Cx(t) + Dz(t) \tag{1b}$$

$$z(t) \in -\mathcal{M}(w(t)). \tag{1c}$$

In this description, $x(t) \in \mathbb{R}^n$ denotes the state variable and $u(t) \in \mathbb{R}^n$ the input at time $t \in \mathbb{R}_{\geq 0}$. We are particularly interested in systems of the form (1) having specific maximal monotonicity properties as will be detailed in the next section. Note that (1) can be perceived as Lur'e-type systems [21] with a set-valued map in the feedback path.

The objective of this paper is to present numerical schemes to construct periodic steady-state solutions (provided they exist) of systems of the form (1) corresponding to periodic input functions $u : \mathbb{R}_{\geq 0} \to \mathbb{R}^n$. These numerical schemes will be accompanied by formal guarantees that the obtained numerical approximations converge to the exact solution (in an appropriate sense) when the discretization parameters converge to specific values. The latter property is referred to as *consistency* of the numerical scheme.

Example 1. In this example, we show that the diode bridge circuit shown in Fig. 1 can be represented by the dynamical system of the form (1). Let x_1 be the current through the inductor L_i, x_2 be the voltage across the capacitor C_o, and u be a sinusoidal voltage source. Let us assume that (z_1, w_1) and (z_4, w_4) are the (current, voltage) pairs of the diodes in the upper part of the bridge and (z_2, w_2) and (z_3, w_3) are the (voltage, current) pairs of the other diodes. By applying the Kirchhoff

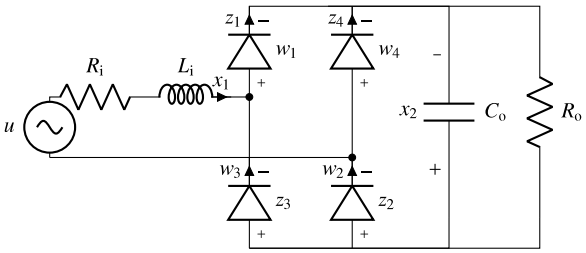

Fig. 1. Power converter diode bridge.

laws to the circuit, one obtains a model in the form (1a)–(1b) with

$$A = \begin{bmatrix} -\frac{R_i}{L_i} & 0 \\ 0 & -\frac{1}{R_o C_o} \end{bmatrix}, \qquad B = \begin{bmatrix} 0 & \frac{1}{L_i} & -\frac{1}{L_i} & 0 \\ \frac{1}{C_o} & 0 & 0 & \frac{1}{C_o} \end{bmatrix}, \tag{2a}$$

$$C = \begin{bmatrix} 0 & 1 \\ 1 & 0 \\ -1 & 0 \\ 0 & 1 \end{bmatrix}, \qquad D = \begin{bmatrix} 0 & 0 & -1 & 0 \\ 0 & 0 & 0 & 1 \\ 1 & 0 & 0 & 0 \\ 0 & -1 & 0 & 0 \end{bmatrix}. \tag{2b}$$

In order to explain the role played by (1c) for the above circuit, let us consider the diode voltage–current (or current–voltage) characteristic. The relation between the current and the voltage of the diodes can ideally be modeled as the maximal monotone mapping in Fig. 2(b), i.e., $z_i(t) \in -\tilde{\mathcal{M}}(w_i(t))$ in which $\tilde{\mathcal{M}}$ given in Fig. 2(b). This means that $z_i(t)$ and $w_i(t)$ are nonnegative and orthogonal for $i = 1, 2, 3, 4$ for each $t \in \mathbb{R}_{\geq 0}$. This can be mathematically written as

$$0 \leq w_i(t) \perp z_i(t) \geq 0 \tag{3}$$

or in vector notation as

$$0 \leq w(t) \perp z(t) \geq 0, \tag{4}$$

where inequalities are interpreted componentwise and $w \perp z = 0$ means that $w^\top z = 0$ for $w, z \in \mathbb{R}^m$. The variables $w(t), z(t)$ satisfying (4) are called complementary variables [36]. As such, (2) together with (4) is in the form (1), where at each time instant t, the condition (1c) is given by (4) and thus $\mathcal{M} : \mathbb{R}^4 \rightrightarrows \mathbb{R}^4$ is the maximal monotone mapping defined as $\mathcal{M}(w) = \tilde{\mathcal{M}}(w_1) \times \tilde{\mathcal{M}}(w_2) \times \tilde{\mathcal{M}}(w_3) \times \tilde{\mathcal{M}}(w_4)$ for $w \in \mathbb{R}^4$. In this particular case, the resulting system is also known as a linear complementarity system, see, e.g., [5,6].

3. Basic properties under maximal monotonicity

In this section, we transform the system (1) into a more classical differential inclusion (DI) formulation, state the conditions we will impose on (1) and discuss the existence and uniqueness of solutions to (1) given an initial state $x(0)$ and an input function $u : \mathbb{R}_{\geq 0} \to \mathbb{R}^n$. Finally, we show the existence and uniqueness of (periodic) steady-state solutions when the system is periodically excited.

3.1. Transformation into classical differential inclusions

To transform (1) into a standard DI formulation, note that $z(t) \in -\mathcal{M}(w(t)) = -\mathcal{M}(Cx(t) + Dz(t))$ can be rewritten as $Cx(t) + Dz(t) \in \mathcal{M}^{-1}(-z(t))$ and thus $Cx(t) \in (\mathcal{M}^{-1} + D)(-z(t))$, which leads to $z(t) \in -(\mathcal{M}^{-1} + D)^{-1}(Cx(t))$. Substituting this expression in (1a), we obtain

$$\dot{x}(t) \in \underbrace{(A - B(\mathcal{M}^{-1} + D)^{-1}C)x(t)}_{-\mathcal{P}(x(t))} + u(t). \tag{5}$$

Interestingly, in [23] it is proven that if (A, B, C, D) in (1) is a passive system with a positive definite storage function (see [23] for the exact definitions) and $\mathcal{M}$ is maximal monotone (next to a minor technical assumption), then $\mathcal{P}$ is maximal monotone as well (possibly after applying a similarity transformation), see [23, Thm. 3] and its proof. If (A, B, C, D) is strictly passive (in the sense of [7]) and $\mathcal{M}$ is maximal monotone, then $\mathcal{P}$ is, in addition, strongly monotone in the sense that there exists a $c > 0$ with

$$\langle x^* - y^* \mid x - y \rangle \geq c|x - y|^2, \tag{6}$$

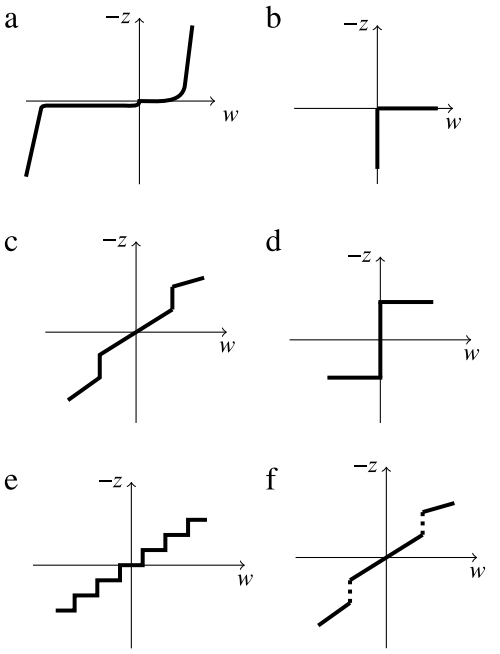

Fig. 2. Typical monotone maps $\mathcal{M}$ from $\mathbb{R}$ to $\mathbb{R}$: (a) current–voltage diode characteristic, (b) complementarity variables, (c) a strongly maximal monotone characteristic, (d) relay, (e) quantizer, (f) a characteristic that is monotone, but not maximal monotone. Note that (a)–(e) are also maximal monotone.

for all $(x, x^*) \in \mathrm{gr}(\mathcal{P})$ and all $(y, y^*) \in \mathrm{gr}(\mathcal{P})$. Throughout the paper, we assume that $\mathcal{P} : \mathbb{R}^n \rightrightarrows \mathbb{R}^n$ is maximal monotone and *strongly monotone* (thereby including the cases just mentioned). Without loss of generality, we can assume that $0 \in \mathcal{P}(x)$ for some x. Indeed, if this would not be the case, we can take a $v \in \mathcal{P}(\tilde{x})$ for some $v, \tilde{x}$ and replace $\mathcal{P}(x)$ by $\mathcal{P}(x) - v$ for all $x \in \mathrm{dom}\, \mathcal{P}$ and $u(t)$ by $u(t) - v$ for all t.

Examples of system (5) satisfying the strong monotonicity assumption include well-known classes of linear complementarity systems [5–10], linear mechanical systems with friction and linear relay systems [11,12], and many others, under strict passivity assumptions on the underlying linear dynamics. Fig. 2 depicts some maximal monotone mappings commonly encountered in practice, thereby showing the range of applications fitting the framework adopted in this paper.

3.2. Solutions and well-posedness

A solution to (5) for a given locally integrable input function $u : \mathbb{R}_{\geq 0} \to \mathbb{R}^n$ is a locally absolutely continuous (AC) function $x : \mathbb{R}_{\geq 0} \to \mathbb{R}^n$ that satisfies (5) almost everywhere. Based on the maximal monotonicity of $\mathcal{P}$, we can prove using the seminal work [3] that for any locally integrable input function $u \in \mathcal{L}_1^{loc}$ there exists a *unique* locally AC solution x to (5) for any $x(0) \in \mathrm{cl}(\mathrm{dom}\, \mathcal{P})$ on $[0, T]$. This can be proven by combining Theorem 3.4 and Proposition 3.8 in [3] together with a reduction argument used in Theorem 1 in [23] (to satisfy $\mathrm{int}\, \mathrm{dom}\, \mathcal{P} \neq \emptyset$ as required in Proposition 3.8 in [3]).

3.3. Contractions and steady-state solutions

The existence and uniqueness discussed in the previous subsection show that for a fixed u we can consider the mapping $x(0) \mapsto x(T)$, which we denote by $\mathcal{T} : \mathrm{cl}(\mathrm{dom}\, \mathcal{P}) \to \mathbb{R}^n$ (assuming u is clear from the context). Interestingly, for $T > 0$ the map $\mathcal{T}$ is a contraction in the sense that there is a $0 \leq \rho < 1$ such that

$$|\mathcal{T}(x) - \mathcal{T}(y)| \leq \rho |x - y|.$$

Indeed, note that the strong monotonicity of $\mathcal{P}$ gives for two different solutions x and y of (5)

$$\begin{aligned} \frac{d}{dt}|x(t) - y(t)|^2 &= 2\langle x(t) - y(t) \mid \dot{x}(t) - \dot{y}(t)\rangle \\ &\leq -2c|x(t) - y(t)|^2 \end{aligned}$$

almost everywhere. Hence, using Grönwall's lemma, we obtain for all $t \in \mathbb{R}_{\geq 0}$

$$|x(t) - y(t)|^2 \leq e^{-2ct}|x(0) - y(0)|^2 \tag{7}$$

thereby establishing the contractivity of $\mathcal{T}$ with $\rho = e^{-cT}$.

Remark 1. Strong links exist between maximal/strong monotonicity and incremental stability [29] (using quadratic Lyapunov functions) and quadratic convergence [31]. For instance, for a system $\dot{x} = f(x, u)$ the latter requires the existence of a positive definite matrix P and an $\varepsilon > 0$ such that $\frac{d}{dt}|x(t) - y(t)|_P^2 = 2(x(t) - y(t))^\top P[f(x(t), u(t)) - f(y(t), u(t))] \leq -\varepsilon|x(t) - y(t)|_P^2$. This is a strong monotonicity requirement on the function $-f$ using the inner product $\langle \cdot \mid \cdot \rangle_P$ given by $\langle v \mid w \rangle_P = v^\top P w$ for $v, w \in \mathbb{R}^n$ (or on the usual inner product after a similarity transformation of the form $z = P^{\frac{1}{2}}x$). As a mapping from time 0 to time T, this leads to a contraction. Note also that, conversely, maximal monotonicity of DIs was used to derive (quadratic) convergence properties in, e.g., [32,33].

Interestingly, the fact that $\mathcal{T}$ is a contraction and $\mathrm{cl}(\mathrm{dom}\,\mathcal{P})$ is invariant under $\mathcal{T}$, i.e. $\mathcal{T}(\mathrm{cl}(\mathrm{dom}\,\mathcal{P})) \subset \mathrm{cl}(\mathrm{dom}\,\mathcal{P})$, immediately gives via the Banach fixed point theorem that there is a *unique* $\bar{x} \in \mathrm{cl}(\mathrm{dom}\,\mathcal{P})$ such that $\mathcal{T}(\bar{x}) = \bar{x}$. Hence, if u is a locally integrable function, that is periodic with period T (i.e., $u(t) = u(t+T)$ for all $t \in \mathbb{R}_{\geq 0}$), exactly one periodic solution exists with period T, denoted by $x_{\mathrm{per}} : \mathbb{R}_{\geq 0} \to \mathbb{R}^n$ assuming again that u is clear from the context. Hence, this reasoning recovers a result that was already established in [3, Thm. 3.14]. In addition, based on (7) we obtain that any other trajectory of the system is converging to this periodic solution when time goes to infinity, and, in fact, the T-periodic solution x_{per} is globally exponentially stable (GES) in the sense that there exist constants $b, c > 0$ such for any solution x to (5) with input u (and thus $x(0) \in \mathrm{cl}(\mathrm{dom}\,\mathcal{P})$) it holds that

$$|x(t) - x_{\mathrm{per}}(t)| \leq be^{-ct}|x(0) - x_{\mathrm{per}}(0)|, \quad t \in \mathbb{R}_{\geq 0}, \tag{8}$$

which shows the exponential convergence of $x(t)$ to $x_{\mathrm{per}}(t)$ when $t \to \infty$. Indeed, if we take $y = x_{\mathrm{per}}$ in (7), we obtain (8) for $b = 1$ and c as in (6).

4. Two numerical schemes

The observations made at the end of the previous section and, in particular, the global exponential stability of the T-periodic solution x_{per} hint upon one way of numerically approximating the periodic solution by "just" simulating the system sufficiently long to approximate the steady-state solution sufficiently well. However, an integration routine is needed to solve the DI (5). Here, we use time-stepping methods [25–27,34,37]. In particular, we will use the backward Euler discretization scheme to get numerical approximations, although extensions to other schemes such as the (θ, γ)-method [37] could be envisioned as well. After providing this time-stepping scheme, we discuss two numerical algorithms for approximating the periodic solution x_{per}. The first one is called the asymptotic simulation (AS) technique and is based on sufficiently long simulation. The second one uses two-point boundary value (2PBV) conditions. A comparison in terms of the required computational time and corresponding approximation accuracy of the two numerical schemes will be provided in Section 6, in which they are both applied for computing the periodic solution of a practical electronic circuit.

4.1. Time-stepping

In this work, we focus on input functions $u : \mathbb{R}_{\geq 0} \to \mathbb{R}^n$ that are T-periodic and of bounded variation on $[0, T]$. Therefore, let us recall the definition of functions of bounded variation.

Let a function $f : [a, b] \to \mathbb{R}^p$ be given for $a < b$. The *total variation* of f on $[a, b]$ is defined by

$$V_f(a, b) := \sup_{\substack{K \in \mathbb{N} \\ a = t_0 < t_1 < \cdots < t_K = b}} \sum_{i=0}^{K-1} |f(t_{i+1}) - f(t_i)|. \tag{9}$$

A function $f : [a, b] \to \mathbb{R}^p$ is said to be *of bounded variation on* $[a, b]$ if $V_f(a, b)$ is finite. Obviously, globally Lipschitz continuous functions are of bounded variation and a function of bounded variation does not need to be continuous. It can be shown that the total variation is additive in the sense that if $c \in (a, b)$ then we have

$$V_f(a, b) = V_f(a, c) + V_f(c, b).$$

This property is useful for the purpose to show that for a given function $u : \mathbb{R}_{\geq 0} \to \mathbb{R}^n$, which is T-periodic and of bounded variation on $[0, T]$ the sequence of approximating (piecewise constant) functions $\hat{u}^h : \mathbb{R}_{\geq 0} \to \mathbb{R}^n$ with $h = \frac{T}{N_h}$ for some $N_h \in \mathbb{N}_{\geq 1}$ defined by

$$\hat{u}^h(t) = u_k^h := u(kh) \quad \text{if } (k-1)h < t \leq kh, \ k \in \mathbb{N}_{\geq 1} \tag{10}$$

and $u^h(0) = u_0^h := u(0)$, converges to u in $\mathcal{L}_1^{loc}$-sense when $N_h \to \infty$ (and thus $h \downarrow 0$). This can be shown as follows:

$$\begin{aligned} |u - \hat{u}^h|_{1,[0,T]} &:= \int_0^T |u(t) - \hat{u}^h(t)|\, dt \\ &= \sum_{k=1}^{N_h} \int_{(k-1)h}^{kh} |u(t) - \hat{u}^h(t)|\, dt \end{aligned}$$

$$
\begin{aligned}
&= \sum_{k=1}^{N_h} \int_{(k-1)h}^{kh} |u(t) - u(kh)|\, dt \\
&\leq h \sum_{k=1}^{N_h} \sup_{t\in[(k-1)h,kh]} |u(t) - u(kh)| \\
&\leq h \sum_{k=1}^{N_h} V_u((k-1)h, kh) \\
&= hV_u(0, T),
\end{aligned} \tag{11}
$$

where we used the definition in (9) in the second inequality. In the last equality we exploited the fact that the total variation is additive. Hence, this also shows that u is locally integrable. Note that due to the periodicity of u, it holds that $u_0^h = u(0) = u(T) = u_{N_h}^h$ and $u_1^h = u(h) = u((N_h+1)h) = u_{N_h+1}^h$ and that $\hat{u}^h : \mathbb{R}_{\geq 0} \to \mathbb{R}^n$ is T-periodic as well.

Consider now an input function $u : \mathbb{R}_{\geq 0} \to \mathbb{R}^n$ that is T-periodic and of bounded variation on $[0, T]$ and let x_{per} be the corresponding periodic solution to (5). Let $\hat{u}^h$ with $h = \frac{T}{N_h}$ for $N_h \in \mathbb{N}_{\geq 1}$ constitute a T-periodic approximating sequence of u as just defined based on (10). Below we only consider values of h equal to $\frac{T}{N_h}$ for some $N_h \in \mathbb{N}_{\geq 1}$, without explicitly mentioning that. Given an initial condition $x(0)$ and defining $x_0^h := x(0)$, we now apply the backward Euler integration scheme to (5) using $\hat{u}^h$ as approximations of u, which gives

$$
\frac{x_k^h - x_{k-1}^h}{h} \in -\mathcal{P}(x_k^h) + u_k^h \tag{12}
$$

with $k \in \mathbb{N}_{\geq 1}$, and

$$
x_k^h \in (I + h\mathcal{P})^{-1}(x_{k-1}^h + hu_k^h) \tag{13}
$$

in which $\mathcal{J}_h := (I + h\mathcal{P})^{-1}$ is the so-called *resolvent*. Interestingly, strong monotonicity of $\mathcal{P}$ leads for all $h > 0$ to the known fact that the *resolvent* $\mathcal{J}_h := (I + h\mathcal{P})^{-1}$ is a *contraction*. For sake of insights and completeness, we recall here the proof, see, e.g., [4,38], which goes as follows: Consider $(x, x^*) \in \text{gr}(\mathcal{P})$ and $(y, y^*) \in \text{gr}(\mathcal{P})$

$$
\begin{aligned}
|x - y + h(x^* - y^*)|^2 &= |x - y|^2 + 2\langle x - y \mid h(x^* - y^*)\rangle + h^2|(x^* - y^*)|^2 \\
&\geq (1 + 2ch)|x - y|^2.
\end{aligned} \tag{14}
$$

This gives that

$$
|x - y| \leq \frac{1}{\sqrt{1 + 2ch}} |\hat{x} - \hat{y}|, \tag{15}
$$

where $x \in \mathcal{J}_h(\hat{x})$ and $y \in \mathcal{J}_h(\hat{y})$, which completes the proof.

Note that this implies that $\mathcal{J}_h$ is single-valued on its domain, and thus we can replace $x \in \mathcal{J}_h(\hat{x})$ by $x = \mathcal{J}_h(\hat{x})$, with some slight abuse of notation. The connection between the strong monotonicity of $\mathcal{P}$ in (5) and the contractivity of $\mathcal{J}_h$ in the corresponding discretization (13) will be instrumental in the sequel. Since $\mathcal{P}$ is maximal monotone, we have that $\text{dom}\, \mathcal{J}_h = \mathbb{R}^n$ (see Theorem 1.2 in [4]). This implies that (13) produces for each h and each function $\hat{u}^h$ and initial state x_0^h a *unique* solution (in discrete-time), and thereby the feasibility of the numerical integration.

We just derived that the resolvent $\mathcal{J}_h$ is a contraction and, in fact, this immediately gives that $x \mapsto \mathcal{J}_h(x + \mu)$ is a contraction for any $\mu \in \mathbb{R}^n$ as well. Since, for fixed $\{u_k^h\}_{k\in\mathbb{N}_{\geq 1}}$ the map $x_0^h \mapsto x_{N_h}^h$ (denoted by $\mathcal{T}_h$, assuming $\{u_k^h\}_{k\in\mathbb{N}_{\geq 1}}$ is clear from the context) is a finite composition of contractions, it is a contraction itself. Hence, there is a unique fixed point $\bar{x}^h$ by (again) applying Banach's fixed point theorem, i.e., there is exactly one $\bar{x}^h$ satisfying

$$
\mathcal{T}_h(\bar{x}^h) = \bar{x}^h. \tag{16}
$$

In a similar way as in the previous section, this shows that the difference inclusion (13) has for each h a unique periodic solution, denoted by $x_{\text{per}}^h : \mathbb{N} \to \mathbb{R}^n$ for each N_h-periodic sequence $\{u_k^h\}_{k\in\mathbb{N}_{\geq 1}}$. To emphasize, note that $x_{\text{per},0}^h, x_{\text{per},1}^h, x_{\text{per},2}^h, \ldots$ denote the values of x_{per}^h at discrete times $k = 0, 1, 2, \ldots$ (complying with actual times $0, h, 2h, \ldots$). In addition, this N_h-periodic solution x_{per}^h is GES due to (15). Hence, this is an important observation as the existence, uniqueness and stability properties of the periodic solution to the difference inclusion (13) (based on contractivity of resolvent $\mathcal{J}_h$) are inherited from the differential inclusions (5) (with maximal/strongly monotone set-valued map $\mathcal{P}$).

Based on the above observations, we are now ready to present the two numerical schemes.

4.2. Asymptotic simulation (AS) method

The first numerical scheme using asymptotic simulation is given in Algorithm 1 and is based on solving the difference inclusion (13) repeatedly.

Algorithm 1. Let $u : \mathbb{R}_{\geq 0} \to \mathbb{R}^n$ be a given T-periodic function of bounded variation on $[0, T]$ and let $\delta > 0$ be a desired approximation tolerance. Select $h > 0$ sufficiently small with $hN_h = T$ for some $N_h \in \mathbb{N}_{\geq 1}$ and choose $x_0^h = x(0)$ assuming the discrete-time input sequence $\{u_k^h\}_{k\in\mathbb{N}_{\geq 1}}$ is obtained as in (10).

- Iterate (13) until $|x^h_{\ell N_h} - x^h_{(\ell-1)N_h}|$ is smaller than the desired tolerance δ for some sufficiently large $\ell \in \mathbb{N}_{\geq 1}$ denoted by ℓ^*.

The approximated T-periodic solution $x_{\mathrm{AS}}^{h,\ell^*} : \mathbb{R}_{\geq 0} \to \mathbb{R}^n$ is now given by piecewise linear interpolation of the points $\tilde{x}_k^h := x^h_{(\ell^*-1)N_h+k}$, $k = 0, 1, \ldots, N_h - 1$ and $\tilde{x}^h_{N_h} := \tilde{x}^h_0$, i.e.,

$$x_{\mathrm{AS}}^{h,\ell^*}(t) = \tilde{x}_k^h + \frac{t - kh}{h}(\tilde{x}^h_{k+1} - \tilde{x}_k^h) \tag{17}$$

for $t \in [kh, (k+1)h)$ and $k = 0, 1, \ldots, N_h - 1$ and then repeated T-periodically.

Algorithm 1 is also written using a meta-language approach in Pseudocode for Algorithm 1 for further clarification.

Pseudocode for Algorithm 1: AS method

Data: $\{T, u, x(0), N_h, \delta, \ell_{\max}\}$, i.e., the period of the input u, the T-periodic input for $t \in [0, T]$, the initial condition, the number of samples, the tolerance, the maximum number of iterations.
Result: AS solution $x^h_{\mathrm{AS}}(t)$
begin
  Set $h = T/N_h$, $\ell = 0$, $x_0^h = x(0)$, and set $\{u_k^h\}_{k=1}^{N_h}$ using (10);
  repeat
    $\ell = \ell + 1$;
    `/* Compute discrete solution */`
    for $k = 1$ **to** N_h **do**
      Compute x_k^h from (13);
    end
    $x^h_{\ell N_h} = x_{N_h}$;
    $e_\ell = |x^h_{\ell N_h} - x^h_{(\ell-1)N_h}|$;
    `/* Re-initialize (13) for next iterations */`
    $x_0^h = x^h_{\ell N_h}$;
  until *($e_\ell \leq \delta$ OR $\ell = \ell_{\max}$)*;
  $\ell^* = \ell$;
  `/* Continuous interpolation by taking the last` N_h `iterations */`
  for $k = 0$ **to** $N_h - 1$ **do**

$$x_{\mathrm{AS}}^{h,\ell^*}(t) = x_k^h + \frac{t - kh}{h}(x^h_{k+1} - x_k^h)$$

    for $t \in [kh, kh + h)$.
  end
end

For this algorithm we will derive some results on the convergence rate, which will turn out to be useful for the consistency proofs later. This will also show that Algorithm 1 terminates in finite time. We already observed that based on (15) showing the contractivity of $\mathcal{J}_h$, we obtain that $\mathcal{T}_h$ is also a contraction satisfying for x, y that

$$|\mathcal{T}_h(x) - \mathcal{T}_h(y)| \leq \left(\frac{1}{\sqrt{1+2ch}}\right)^{\frac{T}{h}} |x - y| \tag{18}$$

as $N_h = \frac{T}{h}$. From this, we obtain that

$$|x^h_{\ell N_h} - \bar{x}^h| \leq \left(\frac{1}{\sqrt{1+2ch}}\right)^{\ell\frac{T}{h}} |\underbrace{x(0)}_{=x_0^h} - \bar{x}^h|, \tag{19}$$

where $x^h_{\ell N_h}$ is computed as in Algorithm 1. Recall that $x(0) = x_0^h$ and $\bar{x}^h$ satisfies (16) and thus $\bar{x}_h = x^h_{\mathrm{per},0}$, where $x^h_{\mathrm{per},k}$ denotes the value of the N_h-periodic solution x^h_{per} to (13) at discrete time step $k \in \mathbb{N}$ (corresponding to actual time kh, as introduced before). Hence, the error $|x^h_{\ell N_h} - \bar{x}^h|$ converges with a rate equal to $(1+2ch)^{-\frac{T}{2h}} < 1$ (over a period T, i.e., N_h discrete-time steps). Note that $\lim_{h\downarrow 0}(1+2ch)^{-\frac{T}{2h}} = e^{-cT}$ being the convergence rate one would obtain from (7) over a time period of

length T, which is equal to the guaranteed convergence rate of $\mathcal{T}$, as expected. Moreover, due to the facts above, we see that for all $e^{-cT} < \gamma < 1$ there is a $\tilde{h} > 0$ such that for all $0 < h < \tilde{h}$ and for $\ell \in \mathbb{N}$ it holds that

$$|x^h_{\ell N_h} - \bar{x}^h| \leq \gamma^\ell |x(0) - \bar{x}^h|, \tag{20}$$

showing also the finite termination of Algorithm 1. The above inequality combined with (18) and $(1 + 2ch)^{-\frac{T}{2h}} \leq 1$ can be used to obtain for all $0 < h < \tilde{h}$ and $\ell^* \in \mathbb{N}_{\geq 1}$ that

$$\max_{k\in\{0,1,\ldots,N_h-1\}} |x^{h,\ell^*}_{\mathrm{AS}}(kh) - x^h_{\mathrm{per},k}| \leq \gamma^{\ell^*-1}|x(0) - \bar{x}^h|. \tag{21}$$

Note that $x^{h,\ell^*}_{\mathrm{AS}}(kh) = \tilde{x}^h_k = x^h_{(\ell^*-1)N_h+k}$, $k = 0, 1, \ldots, N_h - 1$ and that the convergence in Algorithm 1 is towards $\bar{x}^h$ (cf. (20)) and x^h_{per} (cf. (21)). The inequalities derived above will turn out to be useful in the consistency proofs below.

4.3. Two-point boundary value (2PBV) method

As an alternative method to the asymptotic simulation, we can also find the N_h-periodic solution x^h_{per} to (13) by using Algorithm 2, which computes $x^h_{\mathrm{2PBV}} : \mathbb{R}_{\geq 0} \to \mathbb{R}^n$ as the piecewise linear interpolation of x^h_{per}.

Algorithm 2. Let $u : \mathbb{R}_{\geq 0} \to \mathbb{R}^n$ be a given T-periodic function of bounded variation on $[0, T]$. Select $h > 0$ sufficiently small with $hN_h = T$ for some $N_h \in \mathbb{N}_{\geq 1}$ and let the discrete-time input sequence $\{u^h_k\}_{k\in\mathbb{N}_{\geq 1}}$ be obtained as in (10).

- Find the solution $x^h_{\mathrm{per}} : \mathbb{N} \to \mathbb{R}^n$ parameterized by $(x^h_{\mathrm{per},0}, x^h_{\mathrm{per},1}, \ldots, x^h_{\mathrm{per},N_h})$ to the set of inclusions (13) with $k = 0, 1, 2, \ldots, N_h - 1$ and the periodicity constraint $x^h_0 = x^h_{N_h}$.

  The approximated T-periodic solution $x^h_{\mathrm{2PBV}} : \mathbb{R}_{\geq 0} \to \mathbb{R}^n$ is now given by piecewise linear interpolation as

$$x^h_{\mathrm{2PBV}}(t) = x^h_{\mathrm{per},k} + \frac{t - kh}{h}(x^h_{\mathrm{per},k+1} - x^h_{\mathrm{per},k}) \tag{22}$$

for $t \in [kh, (k + 1)h)$ and $k = 0, 1, \ldots, N_h - 1$ and then repeated T-periodically.

The algorithm is also written using a meta-language approach in Pseudocode for Algorithm 2 for further clarification.

Pseudocode for Algorithm 2: 2PBV method

Data: $\{T, u, N_h\}$, i.e., the period of the input u, the exogenous input on the time interval $[0, T]$, the number of samples.
Result: 2PBV solution $x^h_{\mathrm{2PBV}}(t)$
begin
  Set $h = T/N_h$ and set $\{u^h_k\}_{k=1}^{N_h}$ from (10) ;
  `/* Define the set of inclusions by collecting (13) with unknowns` $\{x^h_k\}_0^{N_h}$ `*/`
  for $k = 1$ **to** N_h **do**
    Set

$$x^h_k \in \mathcal{J}_h(x^h_{k-1} + hu^h_k) \tag{23}$$

  end
  `/* Periodicity constraint */`

$$x^h_0 = x^h_{N_h} \tag{24}$$

  Compute $\{x^h_k\}_0^{N_h}$ by solving together the N_h equations (23) with (24) ;
  `/* Continuous interpolation */`
  for $k = 0$ **to** $N_h - 1$ **do**

$$x^h_{\mathrm{2PBV}}(t) = x^h_k + \frac{t - kh}{h}(x^h_{k+1} - x^h_k)$$

    for $t \in [kh, kh + h)$.
  end
end

4.4. Discussion on the two schemes

Let us briefly comment on the two numerical schemes presented above. The AS scheme can be seen as approximating $\bar{x}_h \in \mathbb{R}^n$ (and $x^h_{\text{per}} : \mathbb{N} \to \mathbb{R}^n$) via the limit $\lim_{\ell\to\infty} \mathcal{T}_h^\ell(x_0^h)$. This corresponds to the basic iterations used in Banach's fixed point theorem. The corresponding T-periodic approximation $x^{h,\ell^*}_{\text{AS}} : \mathbb{R}_{\geq 0} \to \mathbb{R}^n$ of the T-periodic solution $x_{\text{per}} : \mathbb{R}_{\geq 0} \to \mathbb{R}^n$ is obtained by piecewise linear interpolation as in (17). The 2PBV scheme directly aims at constructing $\bar{x}_h \in \mathbb{R}^n$ (and thus $x^h_{\text{per}} : \mathbb{N} \to \mathbb{R}^n$) by solving the fixed point relation $\bar{x}_h = \mathcal{T}_h(\bar{x}_h)$. Also here piecewise linear interpolation as in (22) is used to find the approximation $x^h_{\text{2PBV}} : \mathbb{R}_{\geq 0} \to \mathbb{R}^n$ of the periodic solution x_{per}. A comparison in the application of the two numerical schemes will be provided in Section 6 in which they are applied for the computation of the periodic solution of the electronic circuit introduced in Example 1.

4.5. Back to the Lur'e type formulation

The way to solve (13) depends on the particular structure of $\mathcal{J}_h$ and thus on $\mathcal{M}$. As a particular case fitting the circuit model introduced in Example 1, let us assume that $\mathcal{M}$ is given by a collection of complementarity conditions as in Fig. 2(b). In this case w and z are vectors of complementary variables and (1c) can be rewritten as

$$0 \leq w(t) \perp z(t) \geq 0 \tag{25}$$

for all $t \in \mathbb{R}_{\geq 0}$. The discretized version of (1) can then be written as

$$\frac{x^h_k - x^h_{k-1}}{h} = Ax^h_k + Bz^h_k + u^k_k \tag{26a}$$

$$w^h_k = Cx^h_k + Dz^h_k \tag{26b}$$

$$0 \leq w^h_k \perp z^h_k \geq 0 \tag{26c}$$

with $k \in \mathbb{N}$. Solving x^h_k from (26a) leads to

$$x^h_k = \frac{1}{h}F_h x^h_{k-1} + F_h u^h_k + F_h B z^h_k \tag{27a}$$

$$w^h_k = \frac{1}{h}CF_h x^h_{k-1} + CF_h u^h_k + (CF_h B + D)z^h_k \tag{27b}$$

$$0 \leq w^h_k \perp z^h_k \geq 0, \tag{27c}$$

with $F_h = \left(\frac{1}{h}I - A\right)^{-1}$. In this case (26) can be written as (27a) together with

$$0 \leq \frac{1}{h}CF_h x^h_{k-1} + CF_h u^h_k + (CF_h B + D)z^h_k \perp z^h_k \geq 0, \tag{28}$$

which can be solved as a LCP [36] for each $k \in \mathbb{N}_{\geq 1}$ and for a given x^h_0 and $\{u^h_k\}_{k\in\mathbb{N}_{\geq 1}}$. This is exactly the application of Algorithm 1 assuming a periodic input $\{u^h_k\}_{k\in\mathbb{N}_{\geq 1}}$.

The use of Algorithm 2 follows from collecting all (27) for $k = 1, 2, \ldots, N_h$ together with the periodicity condition $x^h_0 = x^h_{N_h}$. Then z^h_k for $k = 1, \ldots, N_h$ are computed as a solution of a 'big' LCP (with additional equality constraint due to periodicity) and these samples are used in (27a) for obtaining x^h_{per} (restricted to $\{0, 1, \ldots, N_h\}$). Several numerical solvers are available for this type of complementarity problem. In fact, in the numerical example we will use the PATH solver [39], which turned out to be very efficient to solve such LCPs with large dimensions.

5. Theoretical guarantees

The main formal guarantees on the numerical schemes derived in this paper are summarized in the next theorem.

Theorem 1. *Consider system (5) with $\mathcal{P}$ maximal monotone and strongly monotone. Let u be T-periodic input and of bounded variation on $[0, T]$ with $T > 0$, and x_{per} the corresponding T-periodic solution. Let x^{h,ℓ^*}_{AS} denote the AS solution obtained with Algorithm 1 and x^h_{2PBV} the 2PBV solution obtained with Algorithm 2. The AS and the 2PBV algorithms are consistent in the sense that*

- *x^{h,ℓ^*}_{AS} converges uniformly to x_{per} when $h \downarrow 0$ and $\ell^* \to \infty$, and*
- *x^h_{2PBV} converges uniformly to x_{per} when $h \downarrow 0$.*

Note that, for notational simplicity, in the formulation of the theorem we did not explicitly write that h is such that $N_h h = T$ for some $N_h \in \mathbb{N}_{\geq 1}$, although these are the only values of h we consider throughout the paper, as mentioned before.

Proof. First we remark that the proof for the consistency of the AS scheme follows from the consistency of the 2PBV method. To see this, note first of all that

$$|x_{\mathrm{AS}}^{h,\ell^*} - x_{\mathrm{per}}|_\infty \leq |x_{\mathrm{AS}}^{h,\ell^*} - x_{\mathrm{2PBV}}^{h}|_\infty + |x_{\mathrm{2PBV}}^{h} - x_{\mathrm{per}}|_\infty, \tag{29}$$

where $|\cdot|_\infty$ denotes the $\mathcal{L}_\infty$-norm. Moreover, by observing the piecewise linear interpolations in (17) and (22), the inequality (21) leads to

$$|x_{\mathrm{AS}}^{h,\ell^*} - x_{2PBV}^{h}|_\infty \leq \gamma^{\ell^*-1}|x(0) - \bar{x}^h| \tag{30}$$

for $\ell^* \in \mathbb{N}_{\geq 1}$ and $0 < h < \tilde{h}$ with $\tilde{h}$ as discussed at the end of Section 4.2. We used here that $x_{\mathrm{2PBV}}^h(kh) = x_{\mathrm{per},k}^h$ for $k = 0, 1, \ldots, N_h$, and that the maximum errors at the interpolation points as in (21) directly translate to $|\cdot|_\infty$-error bounds on the piecewise linear interpolations. Hence, if x_{2PBV}^h converges uniformly to x_{per} (i.e., in $|\cdot|_\infty$-norm) when $h \downarrow 0$, then from (29) and (30) combined we obtain also that $x_{\mathrm{AS}}^{h,\ell^*}$ converges uniformly to x_{per} when $h \downarrow 0$ and $\ell^* \to \infty$. Therefore, in the remainder of the proof we concentrate on the consistency proof for the 2PBV method.

To do so, we are going to consider the set of AC (even Lipschitz continuous) functions $x_{\mathrm{2PBV}}^h : \mathbb{R}_{\geq 0} \to \mathbb{R}^n$, depending on h and we restrict to $[0, T]$ for which we will use for short the notation $\tilde{x}^h : [0, T] \to \mathbb{R}^n$. Note that $\tilde{x}^h$ is obtained as in (22) with $x_{\mathrm{per},0}^h = \bar{x}^h$. If we can show the uniform convergence of $\tilde{x}^h$ to x_{per} (restricted to $[0, T]$) when $h \downarrow 0$, then due to T-periodicity of all involved functions, the proof is complete. Clearly, based on (12) these functions $\tilde{x}^h$ satisfy with $v_k^h := \frac{x_{\mathrm{per},k}^h - x_{\mathrm{per},k-1}^h}{h}$, $k = 1, 2, \ldots, N_h$,

$$\dot{\tilde{x}}^h(t) = v_k^h \in -\mathcal{P}(x_{\mathrm{per},k}^h) + u_k^h, \quad t \in ((k-1)h, kh) \tag{31}$$

and thus

$$\tilde{x}^h(t) = \bar{x}^h + \int_0^t \dot{\tilde{x}}^h(\tau)d\tau \tag{32}$$

for all $t \in [0, T]$.

We are going to exploit the following facts of which the proofs can be found in the Appendix.

Fact 1. *There is a compact set $\Omega \subset \mathbb{R}^n$ with $\bar{x}^h = \tilde{x}^h(0) \in \Omega$ for all $0 < h < 1$.*

Fact 2. *There exist an $M \in \mathbb{R}$ and a $0 < \bar{h} < 1$ such that for all $0 < h < \bar{h}$ and all $k = 1, 2, \ldots, N_h$ it holds that $|v_k^h| \leq M$, where $v_k^h = \frac{x_{\mathrm{per},k}^h - x_{\mathrm{per},k-1}^h}{h}$.*

Fact 2 shows that the collection of $\{\tilde{x}^h\}_h$ is Lipschitz continuous with the same Lipschitz constant M and thus *equicontinuous*. Combining Fact 2 with Fact 1 leads to the conclusion that the collection of $\{\tilde{x}^h\}_h$ is also *uniformly bounded*, i.e., there exists a constant $\hat{M} \in \mathbb{R}$ such that for all h and all $t \in [0, T]$ (in fact for all $t \in \mathbb{R}_{\geq 0}$ due to T-periodicity) $|\tilde{x}^h(t)| \leq \hat{M}$. The celebrated Arzelá–Ascoli theorem gives now a *uniformly convergent* subsequence of $\{\tilde{x}^h\}_h$, whose limit is denoted by $x^{\lim}$. In fact, we will prove that all converging subsequences have the same limit $x^{\lim}$, thereby establishing that the complete sequence itself $\{\tilde{x}^h\}_h$ converges to this limit $x^{\lim}$, which will be shown to be x_{per}.

Take now any converging subsequence of $\{\tilde{x}^h\}_h$ (for simplicity of notation we denote the subsequence also as $\{\tilde{x}^h\}_h$) and denote the limit by $x^{\lim}$. This limit $x^{\lim}$ is also Lipschitz continuous with the same Lipschitz constant and hence almost everywhere differentiable (Rademacher's theorem).

Fact 3. *$x^{\lim}$ is a solution to (5) with input u.*

Since the (sub)sequence $\{\tilde{x}^h\}_h$ converges uniformly to $x^{\lim}$ and $\tilde{x}^h(0) = x_{\mathrm{per},0}^h = x_{\mathrm{per},N_h}^h = \bar{x}^h = \tilde{x}^h(T)$, we obtain that $x^{\lim}(0) = x^{\lim}(T) = \lim_{h\downarrow 0} \bar{x}^h$. Hence, $x^{\lim}$ is a T-periodic solution to (5). However, we must have that $x^{\lim} = x_{\mathrm{per}}$ as there is only one T-periodic solution. Hence, each converging subsequence of $\{\tilde{x}^h\}_h$ converges uniformly to x_{per} and each subsequence of $\{\tilde{x}^h\}_h$ has a uniformly converging subsequence itself due to the Arzelá–Ascoli theorem. This proves that $\{\tilde{x}^h\}_h$ converges uniformly to x_{per}, thereby completing the proof. □

6. Numerical example

Let us reconsider the power converter in Fig. 1, whose dynamical formulation is derived in Example 1. The linear system given by the matrices (A, B, C, D) in (2) can be proved to be strictly passive. Since $\mathcal{M}$ is maximal monotone, $\mathcal{P}$ is strongly monotone and there exists a unique locally AC periodic solution when periodically excited.

The following parameters are considered: $L_{\mathrm{i}} = 0.1$ mH, $R_{\mathrm{i}} = 1$ mΩ, $R_{\mathrm{o}} = 100$ Ω, $C_{\mathrm{o}} = 0.8$ mF and u is a sinusoidal input with frequency $f = 1/T = 50$ Hz and amplitude 220 V (*rms*). We show some results in terms of computation

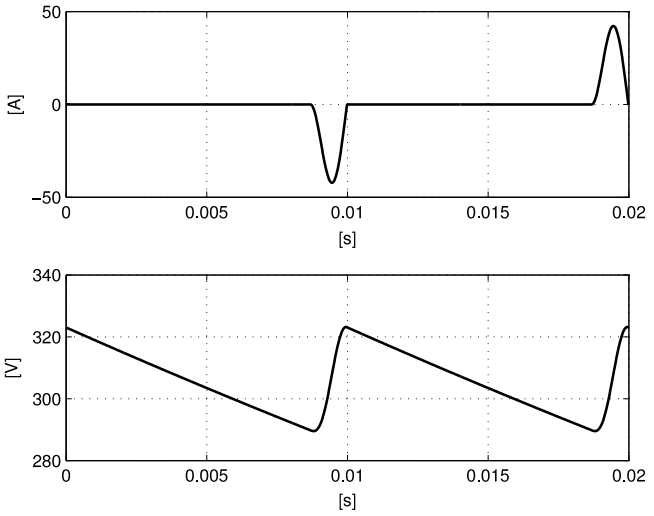

Fig. 3. Steady-state inductor current and output voltage.

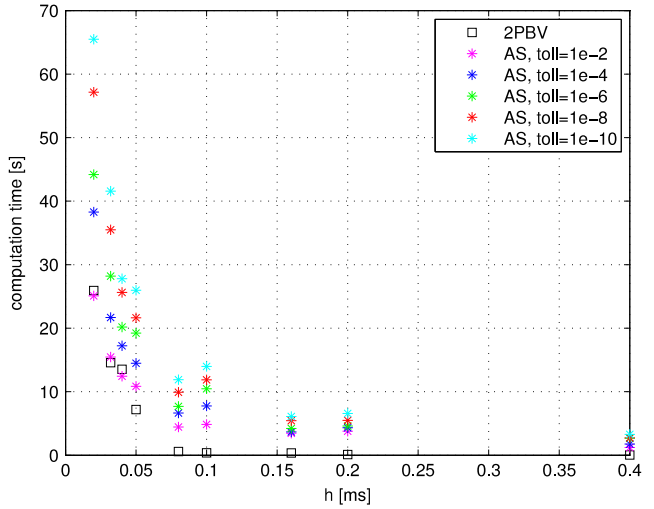

Fig. 4. Computation time necessary to find the periodic steady-state solution by varying h by using the AS method with different values of the tolerance δ and the 2PBV method.

time and approximation accuracy of the numerical schemes presented in Section 4. Both methods have been implemented and executed in MATLAB and complementarity problems are solved by using the PATH solver [39]. When the AS method is used at each time step k a LCP in the form (28) is solved by calling the PATH solver [39]. More details can be found in [16,37]. In Fig. 3, the steady-state inductor current and output voltage are shown when the AS method is used with $h = 0.002$ ms and a tolerance 10^{-14} (computation time 122 s). For the AS method it is necessary to choose a desired tolerance δ that defines the accuracy of the periodic steady-state solution, while the 2PBV method is solved by considering the exact periodicity constraint. In particular, by considering N_h samples in a period T, it is possible to write simultaneously (27) for $k = 1, 2, \ldots, N_h$ ($h = \frac{T}{N_h}$) and use the condition $x_0 = x_{N_h}$. Then the N_h equations can be solved at once by using the PATH solver and a solution for all samples x_k with $k = 0, 1, \ldots, N_h$ can be found as explained in Section 4.5.

Let us make a comparison of the computational burden for the two algorithms. For Algorithm 1, the computational effort clearly depends on the number of iterations for the computed solution to converge to the exact periodic solution within a given tolerance. Instead, for the 2PBV Algorithm the major computational load corresponds to solve the problem (23)–(24) at once. In the particular case of the example, a "big" LCP (with an additional equality constraint) is solved with $4N_h$ (scalar) complementarity conditions. In Fig. 4, the computation time needed for computing the steady-state periodic solution on an Intel Core i7 clocked at 2.40 GHz is shown. The computation time has been computed by increasing the number of samples, N_h, per period, i.e., by decreasing the size of h. Fig. 4 shows that from a computation time point of view, the 2PBV method is more effective than the AS method also when a high numerical accuracy, i.e., $h = 0.02$ ms ($N_h = 10^3$ samples per period) is required.

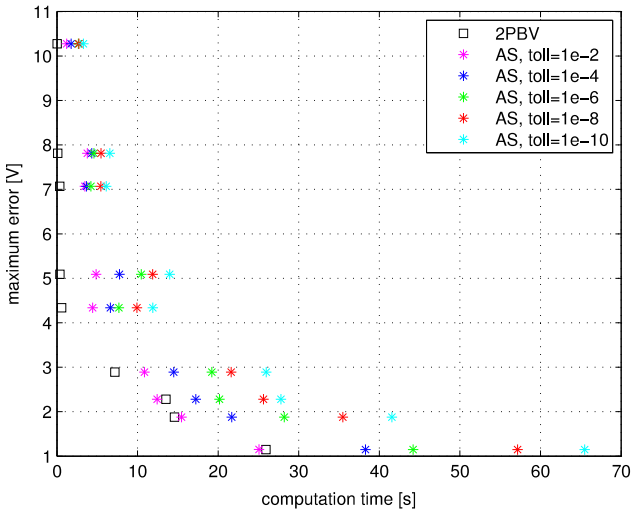

Fig. 5. Maximum error of the steady-state output voltage with respect the 'exact' steady-state solution versus the computation time necessary for the AS method with different values of the tolerance δ and the 2PBV method to find the periodic steady-state solution by varying h.

Now let us consider as the exact periodic solution the one computed by using the AS method with $h = 0.002$ ms and a tolerance of 10^{-14}. Then we can compute the maximum error (in terms of $|\cdot|_\infty$ norm) between this 'exact' solution and the ones obtained by varying h in the AS method with different values of the tolerance and in the 2PBV method, that are x^{h,ℓ^*}_{AS} and x^h_{2PBV}, respectively, and compare these maximum errors with the required computation times. This leads to Fig. 5, which shows that the 2PBV method permits to reach the same accuracy of the AS method, in terms of maximum error, in a smaller computation time. Note also that when h is decreased, the maximum error is decreasing to zero thereby confirming the result of Theorem 1.

7. Conclusions

In the context of Lur'e systems with maximal/strongly monotone mappings in the feedback path, or more general differential inclusions with maximal/strongly monotone maps, we have studied the problem of how to construct periodic solutions when these set-valued systems are periodically excited. We have discussed two numerical schemes based on time-stepping methods. The first method uses asymptotic simulation and the second method is based on solving a 2-point boundary value (2PBV) problem. We have shown the feasibility of the methods in the sense that both methods provide feasible subproblems, i.e., the discretization inherits the existence and uniqueness of periodic solutions from the original system and we have shown their consistency in the sense that in the limit (for the step size converging to zero) the proposed methods recover the exact periodic solution of the original (continuous-time) differential inclusion. Although the results may be expected, we believe it is appropriate and important to formally establish the consistency of the two schemes. Moreover, the proofs reveal valuable information on the numerical schemes. We have compared the two methods on an example of an electrical circuit with ideal diodes showing that the 2PBV method is more effective in the sense that a better approximation accuracy is obtained in a shorter computation time than the asymptotic simulation method for this example.

Appendix

A.1. Proof of Fact 1

Reconsider $x \in \mathbb{R}^n$ with $0 \in \mathcal{P}(x)$. The latter property implies that x is a fixed point for $(I + h\mathcal{P})^{-1}$ and $I + h\mathcal{P}$, i.e. $x \in (I + h\mathcal{P})(x)$ and $x \in (I + h\mathcal{P})^{-1}(x)$. Hence, for a fixed h we obtain from (15) and (13) that

$$|x^h_{\mathrm{per},k} - x| \leq \frac{1}{\sqrt{1+2ch}} |x^h_{\mathrm{per},k-1} - x + hu^h_k|. \tag{A.1}$$

For a fixed h the inequality (A.1) leads to the observation that the set $\mathrm{cl}\, B(x, R_h)$ is positively invariant under (13), where $B(x, R_h)$ is the open ball with center x and radius

$$R_h := \frac{h\tilde{M}}{1 - \sqrt{\frac{1}{1+2hc}}},$$

with $\tilde{M} > 0$ satisfying $|u^h|_\infty \leq \tilde{M}$ for all $h > 0$ and $|u|_\infty \leq \tilde{M}$, which is possible due to u being of bounded variation on $[0, T]$. Indeed, from (A.1) we get

$$|x^h_{\mathrm{per},k} - x| \leq \frac{1}{\sqrt{1+2ch}}|x^h_{\mathrm{per},k-1} - x| + h|u^h_k|.$$

From this it is not hard to see that if $|x^h_{\mathrm{per},k-1} - x| \leq R_h$ then $|x^h_{\mathrm{per},k} - x| \leq R_h$. Hence, this also shows that $\mathrm{cl}\, B(x, R_h)$ is positively invariant under $\mathcal{T}_h$ as $\mathcal{T}_h$ is a finite composition of the maps given through (13).

Since all iterates (i.e., repetitively carrying out $\mathcal{T}_h$) used in the Banach fixed point theorem converge eventually to the unique fixed point being $\bar{x}^h$, we can take a starting iterate $x^h_0 \in \mathrm{cl}\, B(x, R_h)$ and we get that $\bar{x}^h = \lim_{\ell\to\infty}(\mathcal{T}_h)^\ell x^h_0 \in \mathrm{cl}\, B(x, R_h)$. Hence, this provides a bound on $\bar{x}^h$ for a particular h.

Now we can show that all $\bar{x}^h$ are contained in one *common* compact set Ω, because

$$\begin{aligned}\lim_{h\downarrow 0} R_h &= \lim_{h\downarrow 0} \frac{h\tilde{M}}{1 - \sqrt{\frac{1}{1+2hc}}} \\ &= \lim_{h\downarrow 0} \frac{h\sqrt{1+2hc}\tilde{M}}{-1+\sqrt{1+2hc}} \\ &= \frac{\tilde{M}}{c}\end{aligned}$$

where we used L'Hôpital's rule in the last step. This shows that $\{R_h \mid 0 < h < 1\}$ is a bounded set. □

A.2. Proof of Fact 2

To get a uniform bound on $v^h_k = \frac{x^h_{\mathrm{per},k} - x^h_{\mathrm{per},k-1}}{h}$ for all $h > 0$ and all $k = 1, \ldots, N_h$, we can use a reasoning in line with Prop 2.9 and Lemma 2.10 in [4]. Note that, due to (31), we have that (dropping superscripts h and subscripts "per" for notational simplicity)

$$u_k - v_k \in \mathcal{P}(x_k), \quad k \in \{1, \ldots, N_h\}$$

and also

$$u_{k+1} - v_{k+1} \in \mathcal{P}(x_{k+1}), \quad k \in \{1, \ldots, N_h\},$$

where we use that $u_{N_h+1} = u_1$, $v_{N_h+1} := v_1$ and $x_{N_h+1} = x_1$. Using now strong monotonicity of $\mathcal{P}$ gives

$$\langle u_k - v_k + v_{k+1} - u_{k+1} \mid x_k - x_{k+1}\rangle \geq c|x_k - x_{k+1}|^2.$$

From this we obtain by dividing by h that

$$\langle u_k - v_k + v_{k+1} - u_{k+1} \mid v_{k+1}\rangle \leq -c|x_k - x_{k+1}||v_{k+1}|.$$

Hence,

$$|v_{k+1}|^2 \leq \langle v_k \mid v_{k+1}\rangle + \langle u_{k+1} - u_k \mid v_{k+1}\rangle - ch|v_{k+1}|^2$$

and thus

$$\begin{aligned}(1+ch)|v_{k+1}|^2 &\leq \langle v_k \mid v_{k+1}\rangle + \langle u_{k+1} - u_k \mid v_{k+1}\rangle \\ &\leq |v_k||v_{k+1}| + |u_{k+1} - u_k||v_{k+1}|,\end{aligned} \tag{A.2}$$

where we used the Cauchy–Schwarz inequality twice. This leads to (by dividing by $|v_{k+1}|$ when non-zero)

$$|v_{k+1}| \leq \frac{1}{1+ch}(|v_k| + |u_{k+1} - u_k|).$$

As a consequence, we have for $k = 1, 2, \ldots, N_h$ that

$$\begin{aligned}|v_k| &\leq \left(\frac{1}{1+ch}\right)^k |v_0| + \sum_{i=1}^{k}\left(\frac{1}{1+ch}\right)^{k-i+1}|u_i - u_{i-1}| \\ &\leq \left(\frac{1}{1+ch}\right)^k |v_0| + \sum_{i=1}^{k}|u_i - u_{i-1}|.\end{aligned} \tag{A.3}$$

Using now the above inequality for $k = N_h = T/h$ together with $\lim_{h\downarrow 0}\left(\frac{1}{1+ch}\right)^{T/h} = e^{-cT} < 1$, we can find a $\gamma < 1$ and a $\bar{h}$ such that for all $0 < h < \bar{h}$ it holds that

$$|v_{N_h}| \leq \gamma |v_0| + S,$$

with $S = V_u(0, T)$ (note that $u_1^h = u_{N_h+1}^h$). Using now the periodicity of x_{per}^h and x_{2PBV}^h, we get that $v_0 = v_{N_h}$, and thus

$$|v_0| \leq \frac{1}{1-\gamma} S.$$

Hence, from (A.3) we obtain

$$|v_k| \leq \frac{1}{1-\gamma} S + S,$$

for $k = 1, 2, \ldots, N_h$, thereby completing the proof. □

A.3. Proof of Fact 3

Due to Fact 2, the subsequence $\{\dot{\tilde{x}}^h\}_h$ is uniformly bounded, and thus forms a weakly compact set in $\mathcal{L}_2[0, T]$. Using the weak compactness of the set $\{\dot{\tilde{x}}^h\}_h$ in $\mathcal{L}_2[0, T]$ implying that a subsequence of $\{\dot{\tilde{x}}^h\}_h$ converges weakly to a function $v \in \mathcal{L}_2[0, T]$ (and thus v also locally integrable), in combination with the convergence of a subsequence of $\{\bar{x}_h\}_h$ to $\bar{x}'$ (for simplicity of notation we write the subsequence as the complete sequence), we can take limits in (32) to arrive at

$$x^{\lim}(t) = \bar{x}' + \int_0^t v(\tau) d\tau. \tag{A.4}$$

This shows that $v = \dot{x}^{\lim}$, and thus that the (sub)sequence of functions $\{\dot{\tilde{x}}^h\}_h$ converges weakly to $\dot{x}^{\lim} \in \mathcal{L}_2[0, T]$.

To show that $x^{\lim}$ is a solution to (5), we are inspired by the reasoning on page 1126 of [4]. Due to (12) and monotonicity of $\mathcal{P}$ we have for each $(r, r^*) \in \text{gr}(\mathcal{P})$ that for all $\tau \in (kh, (k+1)h)$

$$\langle u^h(\tau) - \dot{x}^h(\tau) - r^* \mid x_k^h - r \rangle \geq 0. \tag{A.5}$$

We now define $x^{h,pc} : [0, T] \to \mathbb{R}^n$ as the piecewise constant functions based on the points $x_{\text{per},k}^h$, $k = 1, \ldots, N_h$, i.e., $x^{h,pc}(t) := x_{\text{per},k}^h$ for $t \in ((k-1)h, kh]$ with $k = 1, \ldots, N_h$ and $x^{h,pc}(0) := x^{h,pc}(T)$. Clearly, due to uniform boundedness of v_k^h (say M the bound as in Fact 2) we have that $|x^{h,pc}(t) - \tilde{x}^h(t)| \leq Mh$ for all t. By integrating (A.5) from s to t with $0 \leq s \leq t \leq T$, we get then that

$$\int_s^t \langle u^h(\tau) - \dot{\tilde{x}}^h(\tau) - r^* \mid x^{h,pc} - r \rangle d\tau \geq 0. \tag{A.6}$$

Now using $|x^{h,pc}(t) - \tilde{x}^h(t)| \leq Mh$ and the fact that $|u^h(\tau) - \dot{\tilde{x}}^h(\tau)|$ is bounded by some $\beta > 0$, we obtain

$$\int_s^t \langle u^h(\tau) - \dot{\tilde{x}}^h(\tau) - r^* \mid \tilde{x}^h - r \rangle d\tau \geq -T\beta Mh. \tag{A.7}$$

Note that

$$\begin{aligned} \frac{1}{2}|\tilde{x}^h(t) - r|^2 - \frac{1}{2}|\tilde{x}^h(s) - r|^2 &= \int_s^t \frac{1}{2}\frac{d}{dt}|\tilde{x}^h - r|^2 d\tau \\ &= \int_s^t \langle \dot{\tilde{x}}^h \mid \tilde{x}^h - r \rangle d\tau, \end{aligned}$$

which gives

$$\frac{1}{2}|\tilde{x}^h(t) - r|^2 - \frac{1}{2}|\tilde{x}^h(s) - r|^2 \leq \int_s^t \langle u^h(\tau) - r^* \mid \tilde{x}^h - r \rangle d\tau + T\beta Mh. \tag{A.8}$$

When $h \downarrow 0$ this gives the inequality (using uniform convergence of x^h to $x^{\lim}$, and $\mathcal{L}_1^{loc}$ convergence of u^h to u, see (11))

$$\frac{1}{2}|x^{\lim}(t) - r|^2 - \frac{1}{2}|x^{\lim}(s) - r|^2 \leq \int_s^t \langle u(\tau) - r^* \mid x^{\lim} - r \rangle d\tau \tag{A.9}$$

for all $(r, r^*) \in \text{gr}(\mathcal{P})$, which shows that $x^{\lim}$ is a so-called *integral solution* (see [40,4]) and thus a (weak and strong) solution to (5) with input u due to Prop. 3.2 and Prop. 3.6 in [3]. □

References

[1] J.P. Aubin, A. Cellina, Differential Inclusions, Springer-Verlag, Berlin, Heidelberg, 1984.
[2] G. Minty, Monotone (nonlinear) operators in Hilbert space, Duke Math. J. 29 (1962) 341–346.
[3] H. Brezis, Operateurs Maximaux Monotones, North-Holland/American Elsevier, Amsterdam, 1973.
[4] J. Peypouquet, S. Sorin, Evolution equations for maximal monotone operators: Asymptotic analysis in continuous and discrete time, J. Convex Anal. 17 (3&4) (2010) 1113–1163.
[5] A.J. van der Schaft, J.M. Schumacher, Complementarity modeling of hybrid systems, IEEE Trans. Automat. Control 43 (4) (1998) 483–490.
[6] W.P.M.H. Heemels, J.M. Schumacher, S. Weiland, Linear complementarity systems, SIAM J. Appl. Math. 60 (2000) 1234–1269.
[7] M.K. Camlibel, W.P.M.H. Heemels, A.J. van der Schaft, J.M. Schumacher, Switched networks and complementarity, IEEE Trans. Circuits Syst. I. Regul. Pap. 50 (2003) 1036–1046.
[8] B. Brogliato, Absolute stability and the Lagrange-Dirichlet theorem with monotone multivalued mappings, Systems Control Lett. 51 (2004) 343–353.
[9] J. Shen, J.S. Pang, Semicopositive linear complementarity systems, Internat. J. Robust Nonlinear 17 (15) (2007) 1367–1386.
[10] F. Vasca, L. Iannelli, M.K. Camlibel, R. Frasca, A new perspective for modeling power electronics converters: Complementarity framework, IEEE Trans. Power Electron. 24 (2) (2009) 456–468.
[11] K.H. Johansson, A. Rantzer, K.J. Astrom, Fast switches in relay feedback systems, Automatica 35 (1999) 539–552.
[12] A. Pogromsky, W.P.M.H. Heemels, H. Nijmeijer, On solution concepts and well-posedness of linear relay systems, Automatica 39 (2003) 2139–2147.
[13] W.P.M.H. Heemels, J.M. Schumacher, S. Weiland, Projected dynamical systems in a complementarity formalism, Oper. Res. Lett. 27 (2) (2000) 83–91.
[14] A. Nagurney, D. Zhang, Projected Dynamical Systems and Variational Inequalities with Applications, Kluwer, Dordrecht, 1996.
[15] B. Brogliato, A. Daniilidis, C. Lemaréchal, V. Acary, On the equivalence between complementarity systems, projected systems and differential inclusions, Systems Control Lett. 55 (2006) 45–51.
[16] V. Sessa, L. Iannelli, F. Vasca, A complementarity model for closed-loop power converters, IEEE Trans. Power Electron. 29 (12) (2014) 6821–6835.
[17] L. Iannelli, F. Vasca, G. Angelone, Computation of steady–state oscillations in power converters through complementarity, IEEE Trans. Circuits Syst. I. Regul. Pap. 58 (6) (2011) 1421–1432.
[18] F. Vasca, L. Iannelli, Dynamics and Control of Switched Electronic Systems, Springer-Verlag, London, 2012.
[19] B. Brogliato, Nonsmooth Impact Mechanics, in: Models, Dynamics and Control, vol. 220, Springer-Verlag London, London, 1996.
[20] M.D.P.M. Marques, Differential Inclusions in Nonsmooth Mechanical Problems, in: Shocks and Dry Friction, vol. 7, Birkhuser, Basel, 1993.
[21] M.R. Liberzon, Essays on the absolute stability theory, Autom. Remote Control 67 (10) (2006) 1610–1644.
[22] B. Brogliato, W.P.M.H. Heemels, Observer design for Lur'e systems with multivalued mappings: A passivity approach, IEEE Trans. Automat. Control 54 (8) (2009) 1996–2001.
[23] M.K. Camlibel, J.M. Schumacher, Math. Program. 157 (2016) 397. http://dx.doi.org/10.1007/s10107-015-0945-7.
[24] A. Dontchev, F. Lempio, Difference methods for differential inclusions: A survey, SIAM Rev. 4 (2) (1992) 263–294.
[25] D.E. Stewart, Time-stepping methods and the mathematics of rigid body dynamics, in: A. Guran, J.A.C. Martins, A. Klarbring (Eds.), Impact and Friction, Birkhäuser, 1999, (Chapter 1).
[26] M.K. Camlibel, W.P.M.H. Heemels, J.M. Schumacher, Consistency of a time-stepping method for a class of piecewise-linear networks, IEEE Trans. Circuits Syst. I. Regul. Pap. 49 (3) (2002) 349–357.
[27] L. Han, A. Tiwari, M.K. Camlibel, J.S. Pang, Convergence of time-stepping schemes for passive and extended linear complementarity systems, SIAM J. Numer. Anal. 47 (5) (2009) 3768–3796.
[28] C. Studer, Numerics of Unilateral Contacts and Friction, Vol. 47, Springer-Verlag, Berlin, Heidelberg, 2009.
[29] D. Angeli, A Lyapunov approach to incremental stability properties, IEEE Trans. Automat. Control 47 (3) (2002) 410–421.
[30] B.P. Demidovich, Lectures on Stability Theory, Nauka, Moscow, 1967, (in Russian).
[31] A. Pavlov, N. van de Wouw, H. Nijmeijer, Uniform Output Regulation of Nonlinear Systems: A Convergent Dynamics Approach, in: Systems and Control: Foundations and Applications (SC) Series, Birkhuser, Basel, 2005.
[32] R.I. Leine, N. van de Wouw, Uniform convergence of monotone measure differential inclusions with application to the control of mechanical systems with unilateral constraints, Internat. J. Bifur. Chaos 18 (5) (2008) 1435–1457.
[33] M.K. Camlibel, N. van de Wouw, On the convergence of linear passive complementarity systems, in: Proceedings of the 46th IEEE Conference on Decision and Control, New Orleans, USA, 2007, pp. 5886–5891.
[34] V. Sessa, L. Iannelli, F. Vasca, V. Acary, A complementarity approach for the computation of periodic oscillations in piecewise linear systems, Nonlinear Dynam. 86 (2) (2016) 1255–1273.
[35] W.P.M.H. Heemels, V. Sessa, F. Vasca, M.K. Camlibel, Time-stepping methods for constructing periodic solutions in maximally monotone set-valued dynamical systems, in: IEEE Conference on Decision and Control, Los Angeles, USA, 2014, pp. 3095–3100.
[36] R.W. Cottle, J.-S. Pang, R.E. Stone, The Linear Complementarity Problem, Academic Press, Inc., Boston, 1992.
[37] V. Acary, B. Brogliato, Numerical Methods for Nonsmooth Dynamical Systems: Applications in Mechanics and Electronics, Vol. 35, Springer-Verlag, London, 2008.
[38] R.T. Rockafellar, R.J.-B. Wets, Variational Analysis, Springer-Verlag, Berlin, Heidelberg, 1998.
[39] S.P. Dirkse, M.C. Ferris, The PATH solver: a non-monotone stabilization scheme for mixed complementarity problems, Optim. Methods Softw. 5 (1995) 123–156.
[40] P. Bénilan, Equations d'Évolution dans un Espace de Banach Quelconque et Applications, Thèse, Orsay, 1972.